Open Research Online

Density and Charge of Pristine Fluffy Particles from Comet 67P/Churyumov–Gerasimenko

Journal Item

oro.open.ac.uk

DENSITY AND CHARGE OF PRISTINE FLUFFY PARTICLES FROM COMET 67P/CHURYUMOV–GERASIMENKO

M. Fulle[1], V. Della Corte[2], A. Rotundi[2,3], P. Weissman[4], A. Juhasz[5], K. Szego[5], R. Sordini[2], M. Ferrari[2,3], S. Ivanovski[2], F. Lucarelli[3], M. Accolla[2,3], S. Merouane[6], V. Zakharov[7], E. Mazzotta Epifani[8,9], J. J. López- Moreno[10], J. Rodríguez[10], L. Colangeli[11], P. Palumbo[2,3], E. Grün[12], M. Hilchenbach[6], E. Bussoletti[3], F. Esposito[8], S. F. Green[13], P. L. Lamy[14], J. A. M. McDonnell[13,15,16], V. Mennella[8], A. Molina[17], R. Morales[10], F. Moreno[10], J. L. Ortiz[10], E. Palomba[2], R. Rodrigo[18,19], J. C. Zarnecki[13,19], M. Cosi[20], F. Giovane[21], B. Gustafson[22], M. L. Herranz[10], J. M. Jerónimo[10], M. R. Leese[13], A. C. López- Jiménez[10], AND N. Altobelli[23]

[1] INAF-Osservatorio Astronomico, Via Tiepolo 11, I-34143 Trieste, Italy; fulle@oats.inaf.it
[2] INAF Istituto di Astrofisica e Planetologia Spaziali, Via Fosso del Cavaliere, 100, I-0133 Rome, Italy
[3] Dip. di Scienze e Tecnologie, Universitá degli Studi di Napoli Parthenope, CDN IC4, I-80143 Naples, Italy
[4] Planetary Science Section, Jet Propulsion Laboratory, 4800 Oak Grove Drive, Pasadena, CA 91109, USA
[5] Wigner Research Centre for Physics, Budapest, Hungary
[6] Max-Planck-Institut für Sonnensystemforschung, Justus-von-Liebig-Weg, 3, D-37077 Göttingen, Germany
[7] LESIA, Obs. de Paris, CNRS, Univ Paris 06, Univ. Paris-Diderot, 5 place J. Janssen, F-92195 Meudon, France
[8] INAF Osservatorio Astronomico di Capodimonte, Salita Moiariello, 16, I-80133 Naples, Italy
[9] INAF Osservatorio Astronomico di Roma, Via di Frascati, 33, Monte Porzio Catone, Rome, Italy
[10] Instituto de Astrofísica de Andalucía (CSIC), Glorieta de la Astronomía s/n, E-18008 Granada, Spain
[11] ESA-ESTEC, Keplerlaan 1, NL-2201 AZ Noordwijk, The Netherlands
[12] Max-Planck-Institut fuer Kernphysik, Saupfercheckweg 1, D-69117 Heidelberg, Germany
[13] Planetary and Space Sciences, Department of Physical Sciences, The Open University, Milton Keynes MK7 6AA, UK
[14] Laboratoire d'Astrophysique de Marseilles, UMR 7326, CNRS & Aix Marseille Université, F-13388 Marseilles Cedex 13, France
[15] The University of Kent, Canterbury, Kent CT2 7NZ, UK
[16] UnispaceKent, Canterbury, Kent CT2 8EF, UK
[17] Departamento de Fsica Aplicada, Universidad de Granada, Facultad de Ciencias, Avda. Severo Ochoa, s/n, E-18071 Granada, Spain
[18] Centro de Astrobiologia (INTA-CSIC), E-28691 Villanueva de la Canada, Madrid, Spain
[19] International Space Science Institute, Hallerstrasse 6, CH-3012 Bern, Switzerland
[20] Selex-ES, Via A. Einstein, 35, I-50013 Campi Bisenzio (Firenze), Italy
[21] Virginia Polytechnic Institute and State University, Blacksburg, VA 24061, USA
[22] University of Florida, Gainesville, FL 32611, USA
[23] ESA-ESAC, Camino Bajo del Castillo, s/n, Urb. Villafranca del Castillo, E-28692 Villanueva de la Canada, Madrid, Spagna

ABSTRACT

The Grain Impact Analyzer and Dust Accumulator (GIADA) instrument on board ESA's *Rosetta* mission is constraining the origin of the dust particles detected within the coma of comet 67 P/Churyumov–Gerasimenko (67P). The collected particles belong to two families: (i) compact particles (ranging in size from 0.03 to 1 mm), witnessing the presence of materials that underwent processing within the solar nebula and (ii) fluffy aggregates (ranging in size from 0.2 to 2.5 mm) of sub-micron grains that may be a record of a primitive component, probably linked to interstellar dust. The dynamics of the fluffy aggregates constrain their equivalent bulk density to $< 1 \, \mathrm{kg \, m^{-3}}$. These aggregates are charged, fragmented, and decelerated by the spacecraft negative potential and enter GIADA in showers of fragments at speeds $< 1 \, \mathrm{m \, s^{-1}}$. The density of such optically thick aggregates is consistent with the low bulk density of the nucleus. The mass contribution of the fluffy aggregates to the refractory component of the nucleus is negligible and their coma brightness contribution is less than 15%.

Key words: comets: general – comets: individual (67P/Churyumov–Gerasimenko) – space vehicles: instruments

1. INTRODUCTION

From 2014 August 1 to September 15, the Grain Impact Analyzer and Dust Accumulator (GIADA) instrument on board ESA's *Rosetta* Mission (Colangeli et al. 2007; Della Corte et al. 2014) collected compact particles, which constrained 67P's dust mass loss rate and dust/gas ratio at heliocentric distances >3.4 AU (Rotundi et al. 2015). Up to 2015 January 14, GIADA has detected a total of 193 compact particles: 81 by both the GDS (laser curtain) and IS (impact sensor) subsystems (GDS+IS) and 112 by IS only. The speed, mass, cross section, and estimates of the bulk density of the GDS+IS particles were retrieved.

Since 2014 mid-September, GIADA has detected showers of GDS-only events, up to a total of 853 detections from 2014

September 15 to 2015 January 14. The showers, with durations up to 30 s, were composed of one or more low speed particle sub-showers each lasting less than 1 s (Table 1). A standard procedure was followed to exclude artifacts due to instrumental noise. GDS stability is checked every hour using on-board calibrations. The temperature, light emission efficiency, and the noise level are monitored. All these parameters are taken into account for data reduction. GDS thermal behavior is stable. During the cruise phase, several interference tests were performed among instruments, with the spacecraft subsystems and self-interference tests, and any spurious behaviors were identified. Very short duration events, which cannot be caused by dust detections, were identified in cruise phase data. All events with a duration $< 5 \times 10^{-5}$ s are classified as noise and

Table 1
GDS-only Showers with at Least 10 Fragments

Date UT[a]	J[b]	t	j	Min–Max τ	m	q	α[c]
14/09/15	129	11	15	0.04 0.35	7.8	4.4	66
14/10/02	24	6	3	0.05 0.11	1.3	0.8	91
14/10/12	27	4	4	0.02 0.08	1.3	0.9	91
14/10/13	24	0.24	1	…	4.0	1.2	95
14/10/16	45	9	3	0.14 0.31	3.2	1.7	90
14/10/17	86	16	5	0.04 0.80	4.3	2.6	91
14/10/22	11	3.5	2	0.02 0.07	0.4	0.4	89
14/10/25	19	0.11	1	…	0.3	0.5	86
14/10/27	15	3.7	2	0.01 0.25	0.3	0.4	85
14/11/06	12	0.95	1	…	0.2	0.3	112
14/11/12	10	0.16	1	…	0.5	0.4	67
14/11/13	55	31	4	0.04 0.37	9.6	2.8	77
14/12/02	41	9	7	0.02 0.09	1.5	1.3	89
14/12/02	60	13	8	0.01 0.12	1.6	1.7	89
14/12/16	83	9	5	0.10 1.71	3.2	2.7	93
15/01/10	12	0.97	1	…	0.3	0.3	91
15/01/14	11	0.12	1	…	0.3	0.3	93

[a] yy/mm/dd.
[b] Shower of J fragments lasting time t (s) and composed of j sub-showers each lasting for a time τ (s). Each shower brings a total charge of q (10^9 e) and a mass of m (10^{-9} kg).
[c] Phase angle (degrees) at the detection.

removed from the GIADA data. No events with properties resembling the GDS-only showers have ever been observed in four years of clean-room tests on the GIADA ground model.

Compact particles were identified as being formed by minerals processed in the pre-solar nebula which were accreted by comet 67P during formation in the Kuiper Belt and/or in the Uranus–Neptune zone (Rotundi et al. 2015). The GDS-only detections, which are a factor of four more numerous, point to grains with physical properties completely different from those of compact particles. In the following discussion we show that the properties of the GDS-only showers infer equivalent bulk densities that are orders of magnitude lower than for compact particles. These low densities are consistent with fluffy aggregates of primitive, unprocessed dust (Suyama et al. 2008). We also infer which of the two dust groups mainly contributes to the refractory mass and cross section of this Jupiter-family comet nucleus.

2. THE OBSERVATIONS

Figure 1 shows all the particle speeds measured by GDS only, extracted from the number of laser pulses (frequency of 0.1 MHz) intercepted during the particle time of flight through the GDS 3 mm thick laser beam. To infer the uncertainty of the GDS speeds, we compare the GDS speed to the GDS+IS speed for all the GDS+IS events (derived from the flight time over the 10 cm distance from GDS to IS, with estimated uncertainties of 6%). When the GDS speed is lower than 9 m s^{-1}, only 5% of the values differ from the corresponding GDS+IS speed by more than 20%. When the GDS speed is larger than 9 m s^{-1}, 100% of the values differ from the corresponding GDS+IS speed by more than 100%. Only one sample has a GDS+IS speed larger than 9 m s^{-1}. At a typical dust speed of 3 m s^{-1}, the GDS speed is accurate if the particle is observed in at least 90 pulses. If the particle is observed in, e.g., 10 pulses only (e.g., a rotating particle or a particle with a signal close to GDS

sensitivity), the GDS speed is overestimated by a factor of 10 while the measurement of the cross section is still accurate.

Figure 2 (left panel) shows the complete statistics of the observed GDS-only events. The GDS signal was converted into a geometric cross section using calibration curves based on compact amorphous carbon. These were the darkest laboratory analogs that could be used for GDS calibration. Fluffy particles are expected to have a low albedo due to the high number of internal reflections when illuminated by the GDS lasers. With calibration curves based on the brightest available silicates, the geometric cross section would become a factor of three lower and the related dust masses a factor of five lower. Eight percent of the GDS-only detections are single events and cover the whole GDS sensitivity range. They could be porous compact particles with a combination of low equivalent bulk density and low speed, which give a momentum below the IS sensitivity. Ninety-two percent of GDS-only events arrive in showers, probably generated by the fragmentation of bigger fluffy parents. Fluffy particles have a large cross-section/mass ratio, which increases the efficiency of the gas drag. They cannot have a speed escaping the nucleus lower than that of compact particles measured by the GDS+IS systems. This is clearly in conflict with the velocity statistics shown in Figure 1, suggesting that the particles in the showers are decelerated before GIADA detection.

Showers of particles were observed during previous comet flybys (Simpson et al. 1987; Rabinowitz 1988; Green et al. 2004), when the spacecraft speed was orders of magnitude larger than the dust speed. This makes the size of the dust clusters associated with these flyby showers orders of magnitude larger than those observed by GIADA. To explain the observed characteristics of the GDS showers, we have developed a simple model based on electrostatic disruption (Mendis & Horanyi 2013) of fluffy aggregates induced by the spacecraft negative potential (Nilsson et al. 2015). In the following discussion we derive the charge on fluffy aggregates and the forces required to disrupt them and hence show that the observed shower speeds can only be satisfied if the aggregates have very low densities (Suyama et al. 2008).

3. PARTICLE CHARGE

The charge carried by a fluffy particle of radius R and equilibrium potential U_d is

$$q = 4 \pi \epsilon_0 U_d \kappa R \qquad (1)$$

where ϵ_0 is the vacuum permittivity, $\kappa = 1$ for spheres and $\kappa > 1$ for non-spherical or fluffy grains (Auer et al. 2007). The potential of the *Rosetta* spacecraft was measured at $U_{SC} = -10$ V (Nilsson et al. 2015). We assume that this value was measured in the expected plasma density of 2×10^8 m^{-3} and energy of 100 eV. Dust charging models were computed taking into account currents provided by cold solar wind ions and electrons, photoelectrons, coma electrons, and the secondary electrons induced by hot and cold plasma components. These simulations (Figure 3) show that the dust equilibrium potential is set by the electron collection current from the ambient plasma and by the secondary electron current emitted by the dust, which depends on the yield parameter δ_m (Mukai et al. 2001), $2.0 < \delta_m < 2.3$ for compact grains of olivine or graphite (Lin & Joy 2005; Balcon et al. 2012). The yield parameter decreases in time due to surface aging effects (Davies & Dennison 1997). In fluffy particles δ_m is lower than
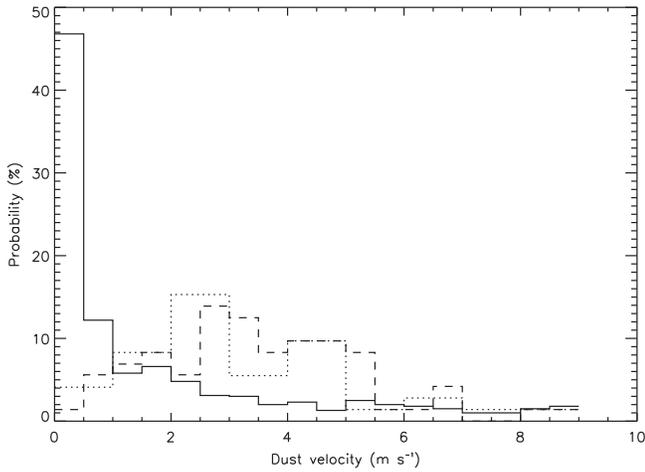
Figure 1. Probability (normalized counts per bin) of particle speeds measured from 2014 August 1 to 2015 January 14. Continuous line: GDS speeds of the single GDS-only events (393 sample; those with speeds >9 m s^{-1} are affected by a large uncertainty and discarded; see the text). Dashed line: GDS+IS speeds (81 samples). Dotted line: GDS speeds of the GDS+IS events (39 samples).

in compact grains because most secondary electrons with an energy of a few eV are ejected toward other parts of the same particle and reabsorbed. Here we consider δ_m as a free parameter, and we fix its value according to the assumed plasma parameters and the measured U_{SC} value.

4. PARTICLE FRAGMENTATION

The tensile strength T in Pa connecting fluffy aggregates is (Guettler et al. 2009; Seizinger et al. 2013)

$$\log_{10} T = 2.8 + 1.4\,\phi, \qquad (2)$$
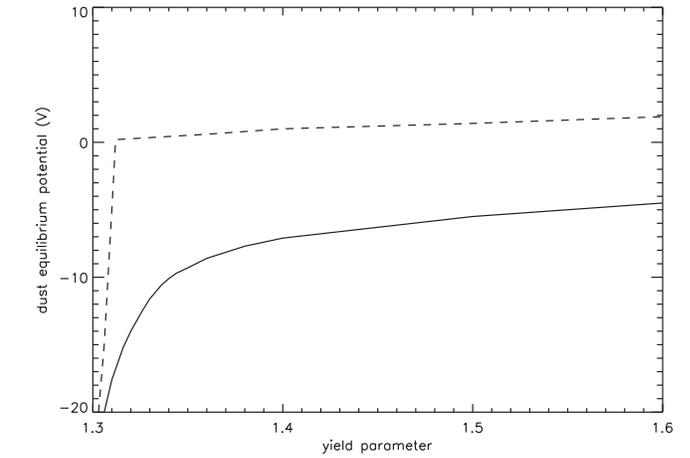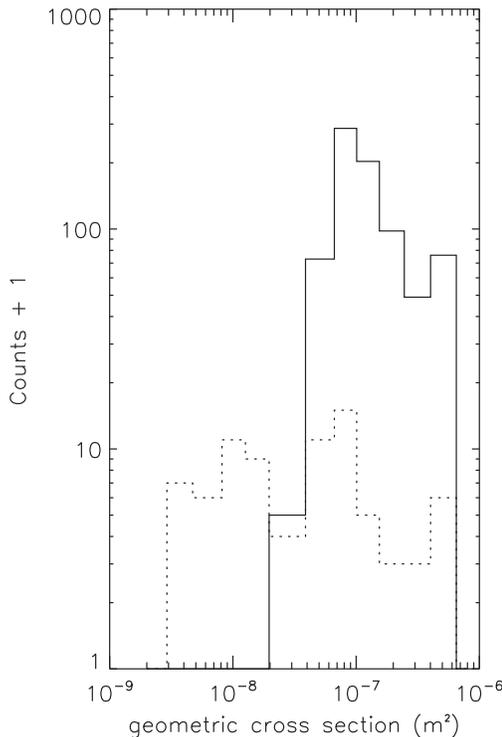
Figure 3. Dust equilibrium potential dependence on the yield parameter δ_m. Dashed line: coma with electrons of 100 eV and space density of 2×10^8 m^{-3}. The continuous line refers to the same coma plasma plus the computed secondary electron flux escaping the spacecraft.

where ϕ is the volume filling factor, $\phi = 3 \times 10^{-4}$ for fluffy particles with bulk density $\rho_d = 3 \times 10^3$ kg m^{-3} and equivalent density $\rho_e = \phi\,\rho_d = 1$ kg m^{-3} (Suyama et al. 2008): we discuss this value in the next section. Equation (2) shows that the aggregates are glued by a tensile strength $T = 0.7$ kPa. The tensile strength due to the internal potential of aggregates of radius $R = 1\,\mu$m and composed of monomers of radius $r = 1$ nm is 7 MPa at $U_d = 5$ V (Auer et al. 2007), and scales as $q^2\,R^{-2}\,r^{-2}$, i.e., as $\left(U_d/r\right)^2$. In real aggregates, monomers do not have the same radius r, so that we define junctions as the smallest monomers linking sub-aggregates of larger monomers.
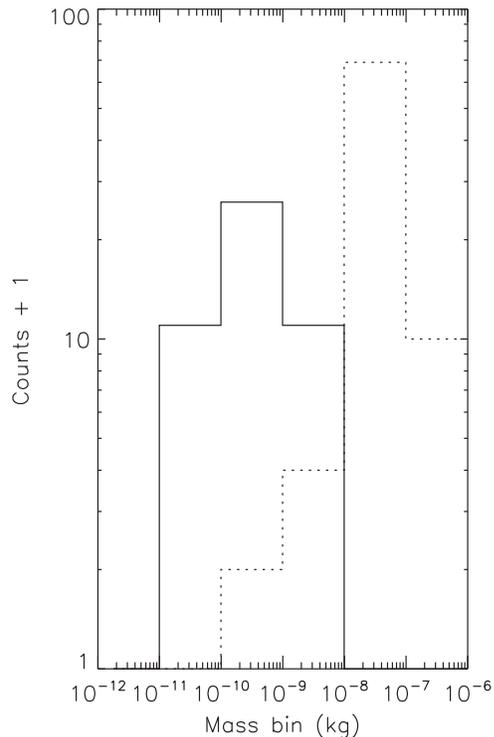
Figure 2. GIADA data from 2014 August 1 to 2015 January 14. Left panel: statistics of 45 GDS-only showers of 784 single events (continuous line) and of 69 GDS-only single particles (dotted line). Right panel: statistics of the integrated mass of 45 GDS-only showers (continuous line) compared to the statistics of 81 GDS+IS events (dotted line).

When the junctions break, the sub-aggregates become fragments. The aggregates may be coated with a sticky organic material, observed on the surface of 67P's nucleus (Capaccioni et al. 2015). This organic coating was observed on interplanetary dust particles collected in Earth's stratosphere (Flynn et al. 2013); it can have a significantly higher tensile strength (Kouchi et al. 2002; Kudo et al. 2002) than is provided by van der Waals forces assumed in Equation (2). The GDS showers offer evidence of fragmentation of aggregates, suggesting that some junctions are not coated by organic material and are linked by van der Waals forces only. At junctions with $r = 0.1\,\mu$m, the electrostatic tensile strength balances the strength gluing the aggregates together (Equation 2). If the fluffy aggregates are composed of N monomers in the spherical envelope of radius R with n monomers along the average line of sight, then $N\pi r^2 = n\pi R^2$ and $N\,4/3\,\pi r^3 = \phi\,4/3\,\pi R^3$, which yields $N = \phi\,(R/r)^3$ and $n = \phi\,R/r$. Most of the fragments observed by GDS have a cross section $\sigma = 8 \times 10^{-8}\,$m^2, i.e., $R = 160\,\mu$m (Figure 2). If $r = 0.1\,\mu$m, then $N = 10^6$ and $n = 1/2$, still consistent with the adopted relationship $\sigma = \pi R^2$.

Far from the spacecraft, $-2 < U_d < +2$ V if $1.31 < \delta_m < 1.6$ (Figure 3, dashed line). Only aggregates with junctions of $r < 40$ nm are fragmented in 67P's coma before approaching the spacecraft (this r value is given by the scaling factor $(U_d/r)^2$). As soon as the aggregates approach the spacecraft, they are charged by the secondary electrons emitted by the spacecraft at $U_{SC} = -10$ V and repelled by its negative potential, so that no electron sheath can form around it (Guillemant et al. 2013). We compute the escape flux of secondary electrons from the spacecraft which is added to the currents charging the grains. The flux of photoelectrons is 2–3 orders of magnitude lower, and neglected. Since these electrons have energies of about 3 eV, they stick on the fluffy aggregates without stimulating secondary electrons from the dust, and bring the aggregate potential to $-17 < U_d < -4.5$ V (Figure 3, continuous line). The charging time in 67P's dense plasma is <0.1 s (Juhasz & Szego 1998). At the same time, the aggregates are disrupted by electrostatic forces until the final fragments are stable against electrostatic disruption with junctions of $r > 0.1\,\mu$m (or even smaller if coated with sticky organic material). The dynamics in the coma of all these charged aggregates are governed both by gas drag, in an almost radial flow until they reach the spacecraft, and by the electric field of 10^{-3} V m^{-1} perpendicular to the solar wind. This effect may explain the high number of detections at phase angles close to 90° (Table 1).

5. PARTICLE DECELERATION

The distribution of fragments from the approaching aggregates has a sharp cut-off at a geometrical cross section $\sigma = 2 \times 10^{-8}\,$m^2 (Figure 2), suggesting a limiting mass that is completely stopped by the spacecraft potential barrier. Smaller fragments are pushed back by this potential and are not detected by GDS although their cross section is still larger than the GDS sensitivity. At distances from the instrument larger than 3 m, we approximate the spacecraft as a cylinder 30 m long and 1 m wide on average; at distances from the payload less than 3 m, the electric field of the surface of the spacecraft pointing to the nucleus dominates that of the solar panels, so that we approximate this surface as a flat disk of radius $R_{PL} = 1$

m. All dust detected by GDS moves along the z-axis, pointing from the instrument to the nucleus (i.e., perpendicular to the disk and to the cylinder long axis and crossing their centers). The spacecraft electric field E_{SC} is

$$E_{SC}(z) = \kappa\,U_{SC}\,R_{SC}\,z^{-1}\left(L^2 + z^2\right)^{-1/2}, \quad z > 3\text{m} \quad (3a)$$

$$E_{SC}(z) = 2\,U_{SC}\,R_{PL}^{-1}\left[1 - z\left(R_{PL}^2 + z^2\right)^{-1/2}\right], \quad z < 3\text{m} \quad (3b)$$

where $L = 15$ m is the distance between $z = 0$ and the tip of each solar panel, $\kappa = 2.5$ (Auer et al. 2007) and $R_{SC} = 1.8$ m is the radius of the sphere of the same volume of the assumed cylinder (Equation (1)). At $z = 3$ m, Equations (3a) and (3b) provide the same electric field $E_{SC} = 1$ V m^{-1}. If we assume $q/m = 1$ C kg^{-1}, the integration of the motion equation $\ddot{z} = E_{SC}(z)\,q/m$ shows that the smallest fluffy fragments are stopped and pushed away from an approaching speed of 6 m s^{-1} within a few centimeters from the GDS sensor. Very few particles have been observed at speeds >6 m s^{-1} (Figure 1). The cross section $\sigma = 2 \times 10^{-8}\,$m^2 corresponds to $R = 80\,\mu$m and to a charge $q = 2 \times 10^{-12}$ C with $\kappa = 20$ (Equation (1)), close to the κ upper limit computed for fluffy aggregates (Auer et al. 2007). In order to obtain a mass $m = 2 \times 10^{-12}$ kg consistent with $q/m = 1$ C kg^{-1}, we require an upper limit of the equivalent density $\rho_e = 1$ kg m^{-3}. Models of proto-planetary dust provided even lower equivalent densities, $\rho_e < 0.1$ kg m^{-3} (Suyama et al. 2008), which imply κ values close to those of spheres ($\kappa = 1$).

The fragmentation occurs close to the GIADA instrument, so that most fragments are collected by the GDS sensor. These are characterized by $\sigma = 8 \times 10^{-8}\,$m^2 (Figure 2) and $q/m = 0.25$ C kg^{-1} (the ratio q/m scales as σ^{-1}) and close to GDS they are decelerated to speeds of a few cm s^{-1} from the expected approaching mean speed of 3 m s^{-1} (Figure 1). All bigger fragments are also decelerated to speeds much lower than those escaping the nucleus. The longest observed durations (up to 30 s, Table 1) become consistent with meter-sized or smaller dust clouds. When the fragment speed becomes lower than the spacecraft speed, large aberration angles affecting the fragment trajectory prevent the fragments crossing GDS to reach the IS sensor: they probably collide and stick on the internal lateral walls of GIADA. All GDS fragments have a momentum below the IS sensitivity (6.5×10^{-10} kg m s^{-1}) when their speed is below 1 m s^{-1}. Table 1 lists the integrated charges and masses of the biggest aggregates, i.e., the sum of the individual charges and masses of all observed fragments per GDS shower, assuming spherical fragments with $\rho_e = 1$ kg m^{-3} and $\kappa = 23$. The largest aggregate carries a charge $q = 4 \times 10^9$ e and has a radius $R = 1.3$ mm. These aggregates are optically thick, $n = \phi\,R/r > 1$.

6. DISCUSSION

We associate the GDS fluffy fragments with the fluffy particles observed by COSIMA (Schulz et al. 2015) by means of the COSISCOPE instrument, providing images of pixel size 14 μm. The morphology of sub-particles smaller than 30 μm cannot be determined. Since the GDS fragments of density $\rho_e = 1$ kg m^{-3} are optically thick, the building blocks of COSISCOPE particles are probably aggregates with this low

density (Rotundi et al. 1998). The impact on the collection plates smashes and collapses the sparse fragments in denser rubble piles. All the fluffy aggregates may be collected in short pulses lasting at most 30 s (Table 1), with a rough frequency of two per week, consistent with the exposure time (one week) of the collection plates. The size of the GDS showers is smaller than the distance between the COSIMA and GIADA instruments, so that we do not expect any time correlation between the GDS and COSIMA showers. The fragmentation of fluffy aggregates as they approach the spacecraft, and further at impact on the collection plates, implies that the size distribution of fluffy particles inferred from COSISCOPE data is steeper than that measured by GIADA at the nucleus surface (Rotundi et al. 2015).

Compact particles larger than 10^{-5} m carry a lower charge, given by Equation (1) with κ of the order of unity (Auer et al. 2007) and have a bulk density a factor 10^3 larger than fluffy aggregates. Their dynamics are not affected by coma and spacecraft potentials. Figure 2 (right panel) shows that the dust flux in fluffy dust aggregates (observed by GDS only) is larger than that of compact particles (observed both by GDS and IS sensors) at dust masses lower than 10^{-8} kg. At larger masses, the flux of fluffy aggregates is significantly lower. Fluffy dust aggregates provide a negligible dust mass loss from the nucleus, and have a size distribution steeper than compact particles. They may contribute to resolve the inconsistency between the 67P size distribution observed by GIADA, characterized by a power index of the differential size distribution = −2 (Rotundi et al. 2015), with that observed from ground, characterized by a power index = −3 (Fulle et al. 2010).

The cross sections of fluffy aggregates and compact particles are similar. Since the spacecraft spent most time at the terminator, there is a bias due to Lorentz forces enhancing the flux of charged aggregates. The single particles detected by the OSIRIS cameras (Rotundi et al. 2015; Sierks et al. 2015) have a probability of <15% of being fluffy (45 fluffy aggregates versus 262 compact particles). If their flux will significantly increase, fluffy particles of equivalent density $\rho_e < 1\,\mathrm{kg\,m^{-3}}$ could be invoked to explain the nucleus density of $470\,\mathrm{kg\,m^{-3}}$ (Sierks et al. 2015). This ρ_e value characterizes aggregates that underwent no processing since they were formed in the presolar nebula. Some particles approaching the *Stardust* spacecraft (Brownlee et al. 2006) could have had a similar low density: they could have fragmented into the denser collected grains following a process similar to that discussed in this paper. *Rosetta* dust collectors are sampling both very pristine fluffy aggregates and compact particles with a bulk density from 800 to $3 \times 10^3\,\mathrm{kg\,m^{-3}}$ (Rotundi et al. 2015) and coming from the inner solar system.

REFERENCES

Auer, S., Kempf, S., & Grün, E. 2007, in Workshop on Dust in Planetary Systems, ed. H. Kruger, & A. Graps (ESA SP-643; Noordwijk: ESTEC), 177
Balcon, N., Payan, D., Belhaj, M., Tondu, T., & Inguimbert, V. 2012, ITPS, 40, 282
Brownlee, D., Tsou, P., Aleon, J., et al. 2006, Sci, 314, 1711
Capaccioni, F., Coradini, A., Filacchione, G., et al. 2015, Sci, 347, aaa0628
Colangeli, L., Lopez-Moreno, J. J., Palumbo, P., et al. 2007, SSRv, 128, 803
Davies, R. E., & Dennison, J. R. 1997, JSpRo, 34, 571
Della Corte, V., Rotundi, A., Accolla, M., et al. 2014, JAI, 3, 1350011
Flynn, G. J., Wirick, S., & Keller, L. P. 2013, EP&S, 65, 1159
Fulle, M., Colangeli, L., Agarwal, J., et al. 2010, A&A, 522, A63
Green, S. F., McDonnell, J. A. M., McBride, N., et al. 2004, JGR, 109, E12S04
Guettler, C., Krause, M., Geretshauser, R. J., Speith, R., & Blum, J. 2009, ApJ, 701, 130
Guillemant, S., Genot, V., Mateo-Velez, J.-C., et al. 2013, ITPS, PP, 99
Juhasz, A., & Szego, K. 1998, JGR, 103, 12015
Kouchi, A., Kudo, T., Nakano, H., Arakawa, M., & Watanabe, N. 2002, ApJL, 566, L121
Kudo, T., Kouchi, A., Arakawa, M., & Nakano, H. 2002, M&PS, 37, 1975
Lin, Y., & Joy, D. C. 2005, SurIA, 37, 895
Mendis, D. A., & Horanyi, M. 2013, RvGeo, 51, 53
Mukai, T., Blum, J., Nakamura, A. M., Johnson, R. E., & Havnes, O. 2001, in Interplanetary Dust, ed. E. Grün, B. A. S. Gustafson, S. F. Dermott, & H. Fechtig (Berlin: Springer), 445
Nilsson, H., Stenberg Wieser, G., Behar, E., et al. 2015, Sci, 347, aaa0571
Rabinowitz, D. L. 1988, A&A, 200, 225
Rotundi, A., Rietmeijer, F. J. M., Colangeli, L., et al. 1998, A&A, 329, 1087
Rotundi, A., Sierks, H., Della Corte, V., et al. 2015, Sci, 347, aaa3905
Seizinger, A., Speith, R., & Kley, W. 2013, A&A, 559, A19
Schulz, R., Hilchenbach, M., Langevin, Y., et al. 2015, Natur, 518, 216
Sierks, H., Barbieri, C., Lamy, P. L., et al. 2015, Sci, 347, aaa1044
Simpson, J. A., Rabinowitz, D., Tuzzolino, A. J., Ksanfomality, L. V., & Sagdeev, R. Z. 1987, in Diversity and Similarity of Comets, ed. E. J. Rolfe, & B. Battrick (ESA SP-278; Noordwijk: ESTEC), 391
Suyama, T., Wada, K., & Tanaka, H. 2008, ApJ, 684, 1310